Banishing Quasiparticles From Josephson-Junction Qubits: Why and How to do it

K. M. Lang, S. Nam, J. Aumentado, C. Urbina, and John M. Martinis, *Member, IEEE*

***Abstract*—Current-biased Josephson junctions are prime candidates for the realization of quantum bits; however, a present limitation is their coherence time. In this paper it is shown qualitatively that quasiparticles create decoherence. We can decrease the number of quasiparticles present in the junctions by two methods—reducing the creation rate with current shunts and increasing the depletion rate with normal-metal traps. Experimental data demonstrate that both methods are required to significantly reduce the number of quasiparticles and increase the system's coherence. We conclude that these methods are effective and that the design of Josephson-junction qubits must consider the role of quasiparticles.**

***Index Terms*—Andreev reflection, Josephson junction, quantum computation, quasiparticle, qubit, superconducting devices.**

THE quantized energy levels of the current-biased Josephson junction, first observed over fifteen years ago [1], form the basis of several more-recent proposals and experiments [2]–[4] for a Josephson-junction realization of a quantum bit (qubit) [5]. Josephson junctions are promising systems for qubits because of the low dissipation inherent to the superconducting state and the relative ease of scaling to multiple qubits through integrated-circuit fabrication technology [6]. Recent experiments have demonstrated that Josephson-junction qubits can in principle perform the single-qubit basic functions needed for quantum computation- initialization of the state, controlled evolution, and state measurement- with coherence times sufficient for this demonstration [4], [7]–[10]. However, because coherence times must be further increased to perform multiple logic operations in a practical quantum computer, an important area of research is understanding the mechanisms of decoherence.

The purposes of this paper are to experimentally demonstrate that quasiparticles can be a significant source of decoherence in a Josephson qubit and to understand how to minimize their presence and effect[1]. At the low temperatures typically used in Josephson qubit experiments ($\sim$10–50 mK), the *equilibrium* quasiparticle density is computed to be exponentially small. However, because the state measurement procedure produces a voltage across the junction, a significant number of quasiparticles are produced and remain in the system even after the qubit is reset into the zero-voltage state. These quasiparticles, with densities far exceeding the equilibrium value, then cause decoherence, perturbing the proper operation of the qubit.

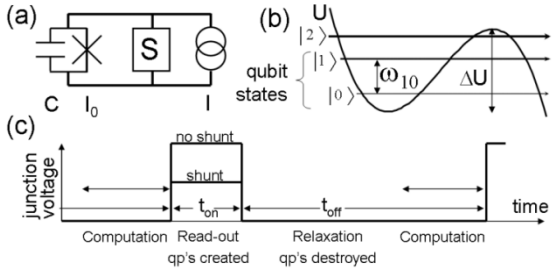

Fig. 1. Josephson-junction qubit operation schematics. (a) Schematic circuit for a current-biased Josephson-junction qubit. 'S' represents the shunt that is used to minimize the generation of quasiparticles. Typical values for the qubits of this paper are $I_o \approx 40\ \mu$A, $C \approx 6$ pF. (b) Cubic potential U as a function of phase across the junction δ derived from an analysis of the circuit of (a). For the qubits in this paper $\omega_{10}/2\pi \approx 7.5$ GHz. (c) Schematic single-qubit quantum-computation cycle showing periods during which quasiparticles (qps) are created and destroyed.

In this paper, we begin with a general overview of the operation of a Josephson qubit. We then give a qualitative picture of how quasiparticles in the junction may affect its operation and cause decoherence. After briefly discussing our particular experimental setup, we consider mechanisms that decrease the production of quasiparticles and increase their rate of removal. Finally, we show experimental data that demonstrate the benefit of reducing the number of quasiparticles for the coherence of the qubit.

Fig. 1 shows a schematic of the circuit for a current-biased Josephson qubit, as well as the resulting effective potential and quantized energy levels [4], [11]. The two lowest energy levels are used for the qubit states. As illustrated in Fig. 1(c), a single-qubit quantum computation generally proceeds as follows. Starting with the qubit in its ground state, a series of current-bias pulses at microwave frequencies are applied to the junction to manipulate the state and hence perform the desired logic operations [12]. At the end of this computation period, the occupation probability of state $|1\rangle$ is measured by inducing a transition of this state out of the potential well. Once out of the well, the phase of the superconductor increases rapidly, which is equivalent to a voltage developing across the junction. This read-out voltage, maintained for a time $t_{\rm on}$, indicates the state of the qubit but also, unfortunately, creates a large number of quasiparticles. After the read-out, the junction is returned to the zero-voltage state for a time $t_{\rm off}$, which permits relaxation of

Manuscript received August 6, 2002. This work is supported in part by the NSA under Contract MOD709001. Contribution of NIST not subject to copyright.

K. M. Lang, S. Nam, J. Aumentado, and J. M. Martinis are with the National Institute of Standards and Technology, Boulder, CO 80305-3328 USA (e-mail: martinis@boulder.nist.gov).

C. Urbina is with Service de Physique de l'Etat Condensé, Commissariat à l'Energie Atomique, Saclay, F-91191 Gif-sur-Yvette Cedex, France.

Digital Object Identifier 10.1109/TASC.2003.814121

[1]Experiments on SET devices have already addressed this issue by incorporating quasiparticle traps in their design. See [9], for example.

both the qubit state toward its ground state and the number of quasiparticles toward zero. When the computation cycle begins again, any remaining quasiparticles may cause decoherence in the next cycle.

Decoherence occurs during the computation period of the qubit cycle, and may be thought of as deviations from the intended trajectory of the qubit state. Such deviations may take two forms: variation in the rate of evolution of the relative phase between the $|0\rangle$ and $|1\rangle$ states and unintended transitions between these states. Decoherence from quasiparticles can arise via either of these channels. For example, quasiparticles tunneling across the junction create shot noise in the current bias. Noise at the qubit transition frequency ω_{10} causes unintended state transitions, whereas noise at low frequencies alters the junction bias current I and hence ω_{10}, leading to unintended variations in the phase evolution [12]. Quasiparticles also affect the critical current I_o of the junction by changing the effective Josephson supercurrent of the conduction channels [13]. Fluctuations in I_o produce decoherence as with bias-current noise. Finally, quasiparticles provide a mechanism for energy dissipation that can result in unintended $|1\rangle \rightarrow |0\rangle$ transitions.

The specific 'phase-qubit' device and operation used to measure quasiparticle induced decoherence for this paper is identical to that previously described [4] with one significant difference. In the previous experiment we used Nb–Al_2O_3–Nb tri-layer junctions, whereas in the present experiment we use Al–Al_2O_3–Al junctions. This change was implemented for two reasons. First, we suspect that fluctuations and dissipation seen in our previous experiment may have arisen from trapping sites in the Nb tri-layer tunnel barrier. Second, other research groups have achieved longer coherence and energy relaxation times with Al junctions [9], [14].

Our new Al junctions were fabricated by a process that should be compatible with making large numbers of qubits in the future, and we describe here in detail the procedure. The junction geometry is illustrated in Fig. 2. Optical photolithography is used for pattern definition of all layers, with the order of deposition and processing as follows. (1) We sputter deposit a 0.1 μm thick Al film to form the base layer of the junction. This film is then patterned by wet etch. (2) A 0.2 μm thick SiO_2 insulating layer is deposited by ECR-PECVD (electron-cyclotron plasma-enhanced chemical vapor deposition). (3) We fabricate the quasiparticle traps by evaporating a 3 nm adhesion layer of Ti followed by 0.1 μm of AuCu (25 wt.% Cu). This layer is patterned with liftoff. (4) The Al Josephson junctions are fabricated by first opening a window in the SiO_2 by reactive-ion etching using CHF_3–O_2 process gases. The Al base electrode is then cleaned by Ar ion milling for one minute at 800 V and at an ion current density 0.15 mA/cm^2. The tunnel barrier is formed by oxidizing in 10 Torr of O_2 for 10 minutes, and the junction is completed by sputtering 0.1 μm of Al for the counter-electrode. This final Al layer is patterned by wet etch. (5) Vias and a wiring layer are deposited using steps identical to (4) but without the oxidation step.

The quality of the tunnel junctions thus fabricated is demonstrated by measurements of their current–voltage $(I$–$V)$ characteristics as shown in Fig. 3. This I–V shows low quasiparticle

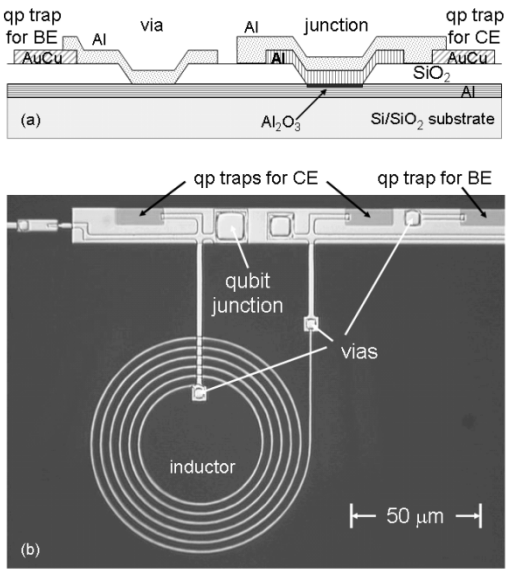

Fig. 2. (a) Schematic cross-section and (b) photomicrograph of our Josephson-junction qubit illustrating the fabrication process and quasiparticle trap geometry. The base electrode (BE) and counter electrode (CE) of the Josephson junction are Al. Quasiparticle (qp) traps are fabricated from AuCu and directly connect to the CE, but connect to the BE through a via.

leakage inside the gap, comparable in magnitude to that reported in the literature [15]. We note that the critical process variable for obtaining low quasiparticle leakage was the ion-mill voltage. Initial devices milled at 200 V–400 V gave very leaky and poor quality junctions. Milling voltages from 600 V to 1000 V produced high quality I–V characteristics like those shown here.

To evaluate the junction I–V, consider the multiple- Andreev-reflection theory of quasiparticle tunneling [16]–[19] which predicts steps in conductance at voltages $2\Delta/ne$ for an order-n tunneling process. The conductance is predicted to decrease by a constant multiplicative factor for each order, with the exact factor depending on the quality of the tunnel barrier. Our data are reasonably consistent with the assumption that most of the tunneling current occurs through a small number of conduction channels that have nearly equal tunneling probability. The I–V of Fig. 3 clearly shows a plateau between 2Δ and Δ, with a relatively large factor of 300 step in conductance. At lower voltages the data are consistent with further significant reductions in conductance.

We now turn to a discussion of the role of quasiparticles in our qubit. We first consider the generation of quasiparticles which occurs when a voltage appears across the junction during the state measurement. One method to minimize the creation of quasiparticles is to limit the time $t_{\rm on}$ the qubit remains in the voltage state. Our electronics presently limit $t_{\rm on}$ to greater than about 50 μs; however, we plan to reduce this time in the next generation of electronics to about 1 μs.

A second method to minimize quasiparticle creation is to place a current shunt in parallel with the junction. Because the rate of quasiparticle creation is proportional to the quasiparticle current $I_{\rm qp}$ flowing through the junction, reducing this current reduces the generation rate. When an unshunted junction switches to the voltage state, $I_{\rm qp}$ is approximately given by the

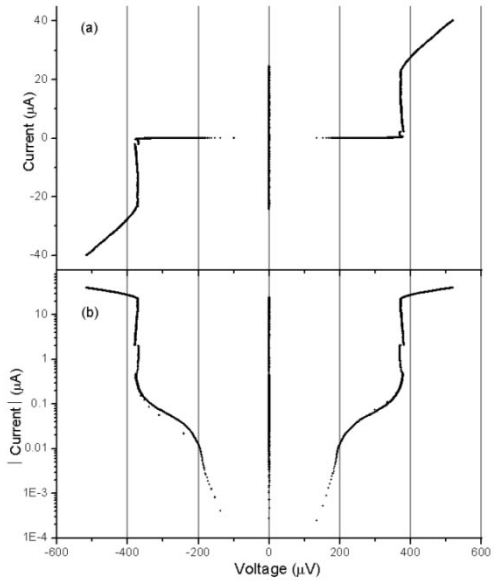

Fig. 3. Current–voltage plots of Al–Al_2O_3–Al junction. (b) is the same plot as (a) but on a logarithmic current scale. The data were taken at 20 mK on a junction of area 100 μm^2. Currents <0.5 μA were taken after reducing the junction supercurrent with a magnetic field. The quasiparticle-current plateau at $\sim$70 nA corresponds to multiple-Andreev-reflections for $n = 2$.

junction critical current which corresponds to a junction voltage of about $2\Delta/e$. By limiting this voltage with a shunt, $I_{\rm qp}$ may be greatly reduced.

In initial trials we tried a resistive shunt but found that, due to retrapping into the zero-voltage state, the qubit junction did not reliably switch into the voltage state. We subsequently tried an Al–Al_2O_3–Cu NIS tunnel junction fabricated with a process similar to the one used for our Al Josephson junctions, but with Cu replacing Al in the last step. The NIS-junction shunt is fabricated on a separate chip and is mounted about 2 cm away from our qubit junction so that quasiparticles created in the shunt cannot diffuse to the qubit junction. The NIS-shunt worked well, presumably because the large differential resistance of the NIS junction near zero voltage removes dissipation and current noise at small voltages when the qubit is likely to retrap. The NIS junction limits the voltage across the qubit junction to $\sim \Delta/e$, significantly reducing the quasiparticle current flowing through it. Referring to the I–V of Fig. 3, the NIS shunt has reduced $I_{\rm qp}$ and hence the rate of quasiparticle creation by a factor of about 1000.

Although the NIS shunt substantially reduces the generation of quasiparticles, there are nonetheless a finite number created. So we must consider mechanisms for removing these remaining quasiparticles. In a superconductor, quasiparticles recombine into Cooper pairs at a rate proportional to their density. At high density this is a rapid depletion mechanism; however, to effectively remove quasiparticles when the density is low, alternative channels for quasiparticle decay must be created. One such channel is a quasiparticle trap that consists of a normal-metal island in good electrical contact with each of the superconducting leads of the Josephson junction. The geometry of the traps we have used is shown in Fig. 2(b). Because the traps appear to the quasiparticles as an effective potential well of depth Δ, when they diffuse to the traps they are captured and dissipate their energy to the normal metal. Provided that the temperature of the normal metal is much less than Δ/k, the normal metal will only be a sink, and not a source of quasiparticles.

We demonstrate the effectiveness of the NIS shunt and quasiparticle traps in reducing the number of quasiparticles with the data of Figs. 4 and 5. In Fig. 4 we plot the escape rate Γ at which the qubit junction switches to the voltage state as a function of applied bias current I. We show data for two relaxation times $t_{\rm off}$, and for two samples- one with both an NIS shunt *and* quasiparticle traps and one with neither. The monotonic increase of Γ with increasing I results from the decrease in the effective potential barrier height ΔU. (See Fig. 1(b).) The peaks are the result of injecting microwaves at a fixed frequency [1], which resonantly increases the escape rate due to $|0\rangle \rightarrow |1\rangle$ transitions. This resonance peak is used as a marker of current to correct for any small drift in the current bias and critical current. The data from Fig. 4 and other such plots are used to measure, for a fixed value of I, a representative escape rate Γ_I. In Fig. 5 we plot this representative escape rate vs. relaxation time $t_{\rm off}$, for four samples representing all combinations of the presence and absence of the NIS shunt and quasiparticle traps. Panels (a) and (b) represent two different duty cycles $t_{\rm on}/t_{\rm off}$. For ease of comparison, we have normalized the data to the rate $\Gamma_{I\rm norm}$ at maximum $t_{\rm off}$ and minimum $t_{\rm on}$.

The escape rates plotted in Figs. 4 and 5 can be used to indicate at least qualitatively the number of quasiparticles in the junction. Quasiparticles produce shot noise in the bias current which can induce upward state transitions. In addition, quasiparticle-induced low-frequency variations in the bias current can effectively lower the potential barrier height ΔU due to the extremely nonlinear dependence of the tunneling probability on that quantity. Both of these quasiparticle induced effects result in an enhanced escape rate. In summary then, given our understanding that quasiparticles produce bias-current noise and that an increase in noise produces an increase in the escape rate, then *an increase in the escape rate implies an increase in the number of quasiparticles.*

Although the four devices are difficult to compare absolutely because they have slightly different critical currents, in Fig. 5 we compare their dependencies on $t_{\rm off}$ for two duty cycles $t_{\rm on}/t_{\rm off}$. The data of Fig. 5 show a much more dramatic increase in the number of quasiparticles at smaller relaxation times $t_{\rm off}$ and higher duty cycles for devices lacking shunts, traps or both. Escape rates that are independent of $t_{\rm off}$ imply a small rate of quasiparticle decay, which arises when fewer quasiparticles remain in the junction. We observe that the escape rate becomes nearly independent of $t_{\rm on}$ and $t_{\rm off}$ for the device with *both* the NIS shunt and quasiparticle trap. We conclude that in order to greatly decrease the number of quasiparticles, our qubit needs a combination of decreased quasiparticle generation with the shunt and more rapid removal of the quasiparticles by the trap.

We now consider how reduced quasiparticle number affects the coherence of the qubit by returning to Fig. 4 and examining the shape of the resonance peaks. The quality factor Q is inversely proportional to the full width at half maximum of the resonance peak [4] and provides a measure of the coherence of

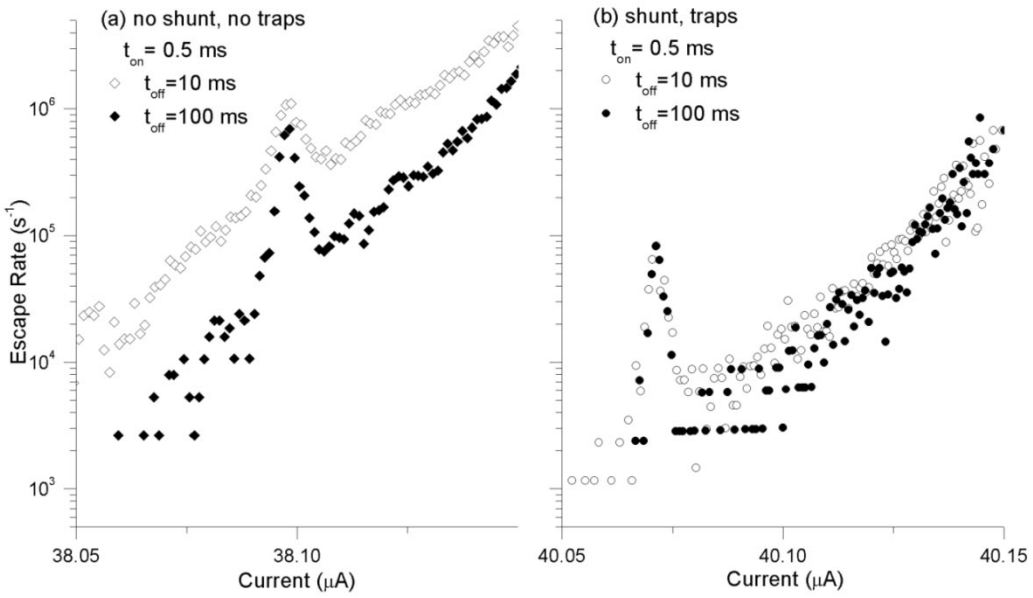

Fig. 4. Escape rate of the qubit to the voltage state Γ vs. junction bias current I for two samples and two relaxation times $t_{\rm off}$. The applied microwave component of the bias current I for (a) and (b) was at 7.2 GHz and 7.5 GHz respectively.

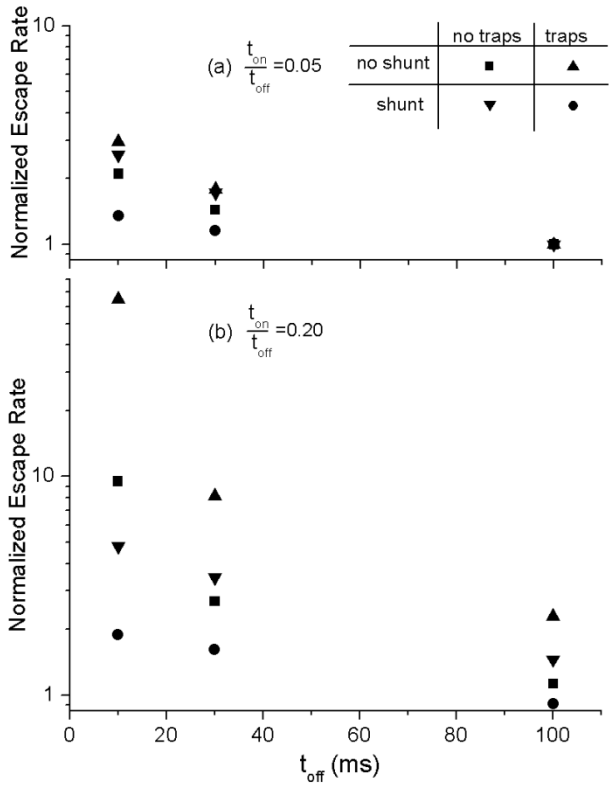

Fig. 5. Normalized escape rate $\Gamma_I/\Gamma_{I\rm norm}$ vs. relaxation time $t_{\rm off}$ for four samples representing all combinations of the presence and absence of the NIS shunt and quasiparticle traps. The normalization value is taken at the rightmost point of (a). The error of the measurement is $\sim 10\%$.

the qubit. We see from the resonance peaks of Fig. 4(a) that for the device with neither shunts nor traps, Q increased with a longer relaxation time and correspondingly lower duty cycle. Comparing the shape of the resonance peaks in Fig. 4(b) to those of Fig. 4(a), for the same relaxation time and duty cycle, the device with both the shunt and traps has a larger Q than the device with neither. Both observations lead us to conclude that fewer quasiparticles give longer coherence times. Although more detailed conclusions must await a quantitative model, our results definitively demonstrate that the NIS shunt and the quasiparticle traps are highly effective in reducing the number of quasiparticles present in the qubit junction, and further that this reduction in quasiparticle number results in longer coherence times for the Josephson qubit.

Although this paper has discussed our initial efforts to reduce the number of quasiparticles, we believe these techniques can be refined further. For example, we can greatly reduce the number of quasiparticles generated by using an NIS junction with an even smaller gap. With greater understanding of the physics of quasiparticle diffusion and trapping, we can also optimize the geometry and size of the traps to more quickly remove the quasiparticles.

We have shown that quasiparticles must be considered in the design of a Josephson-junction qubit. Quasiparticles are created at a greatly reduced rate when we lower the switching voltage by shunting the qubit with a NIS tunnel junction. Quasiparticles are removed at a greatly increased rate when we connect the junction leads to normal metal traps. For our current-biased Josephson junction, we have demonstrated that both shunts and traps are needed in order to reduce the deleterious effects of quasiparticles and that doing so increases the coherence of the Josephson-junction qubit.

ACKNOWLEDGMENT

The authors would like to thank M. Devoret for helpful discussions and N. Bergren for fabrication of the qubit chips.

REFERENCES

[1] J. M. Martinis, M. H. Devoret, and J. Clarke, "Energy-level quantization in the zero-voltage state of a current-biased Josephson junction," *Phys. Rev. Lett.*, vol. 55, pp. 1543–1567, Oct. 1985.

[2] R. C. Ramos, M. A. Gubrud, A. J. Berkley, J. R. Anderson, C. J. Lobb, and F. C. Wellstood, "Design for effective thermalization of junctions for quantum coherence," *IEEE Trans. Appl. Superconduct.*, vol. 11, pp. 998–1001, Mar. 2001.

[3] S. Han, Y. Yu, X. Chu, S.-I. Chu, and Z. Wang, "Time-resolved measurement of dissipation-induced decoherence in a Josephson junction," *Science*, vol. 293, pp. 1457–1459, Aug. 2001.

[4] J. M. Martinis, S. Nam, J. Aumentado, and C. Urbina, "Rabi oscillations in a large Josephson-junction qubit," *Phys. Rev. Lett.*, vol. 89, pp. 117 901/1–4, Sep. 2002.

[5] M. A. Nielsen and I. L. Chuang, *Quantum Computation and Quantum Information*. Cambridge, U.K.: Cambridge University Press, 2000.

[6] Y. Makhlin, G. Schön, and A. Shnirman, "Quantum-state engineering with Josephson-junction devices," *Rev. of Mod. Phys.*, vol. 73, pp. 357–400, Apr. 2001.

[7] Y. Nakamura, C. D. Chen, and J. S. Tsai, "Spectroscopy of energy-level splitting between two macroscopic quantum states of charge coherently superposed by Josephson coupling," *Phys. Rev. Lett.*, vol. 79, pp. 2328–2331, Sep. 1997.

[8] Y. Nakamura, Y. A. Pashkin, A. Yu, and J. S. Tsai, "Charge echo in a cooper-pair box," *Phys. Rev. Lett.*, vol. 88, pp. 047 901/1–4, Jan. 2002.

[9] ——, "Manipulating the quantum state of an electrical circuit," *Science*, vol. 296, pp. 886–889, May 2002.

[10] Y. Yu, S. Han, X. Chu, S.-I. Chu, and Z. Wang, "Coherent temporal oscillations of macroscopic quantum states in a Josephson junction," *Science*, vol. 296, pp. 889–892, May 2002.

[11] J. M. Martinis, M. H. Devoret, and J. Clarke, "Experimental tests for the quantum behavior of a macroscopic degree of freedom: The phase difference across a Josephson junction," *Phys. Rev. B*, vol. 35, pp. 4682–4698, Apr. 1987.

[12] J. M. Martinis, S. Nam, J. Aumentado, K. M. Lang, and C. Urbina, "Decoherence of a superconducting qubit from bias noise," Phys. Rev. B, 2002, submitted for publication.

[13] M. F. Goffman *et al.*, "Supercurrent in atomic point contacts and Andreev states," *Phys. Rev. Lett.*, vol. 85, pp. 170–173, July 2000.

[14] K. W. Lehnert, K. Bladh, L. F. Spietz, P. Delsing, and R. J. Schoelkopf, "Measurement of the excited-state lifetime and coherence time of a microelectronic circuit," Phys. Rev. Lett., 2002, submitted for publication.

[15] M. A. Gubrud *et al.*, "Sub-gap leakage in Nb/AlO_x/Nb and Al/AlO_x/Al Josephson junctions," *IEEE Trans. Appl. Superconduct.*, vol. 11, pp. 1002–1005, Mar. 2001.

[16] G. B. Arnold, "Superconducting tunneling without the tunneling hamiltonian. Ii. Subgap harmonic structure," *J. Low Temp. Phys.*, vol. 68, pp. 1–27, July 1987.

[17] D. Averin and A. Bardas, "AC Josephson effect in a single quantum channel," *Phys. Rev. Lett.*, vol. 75, pp. 1831–1834, Aug. 1995.

[18] J. C. Cuevas, A. Martin-Rodero, and A. L. Yeyati, "Hamiltonian approach to the transport properties of superconducting quantum point contacts," *Phys. Rev. B*, vol. 54, pp. 7366–7379, Sep. 1996.

[19] E. N. Bratus, V. S. Shumeiko, E. V. Bezuglyi, and G. A. B. Wendin, "DC-current transport and ac Josephson effect in quantum junctions at low voltage," *Phys. Rev. B*, vol. 55, pp. 12 666–12 677, May 1997.